EVALUATION OF INFINITE SLOPE STABILITY WITH VARIOUS SOILS UNDER WET-DRY CYCLE

* Depu Hu¹, Shoji Kato² and Byeong-Su KIM³

^{1,2} Graduate School of Engineering, Kobe University, Japan; ³ Department of Civil & Environmental Engineering, Dankook University, Korea

*Corresponding Author, Received: 12 June 2023, Revised: 09 Jan. 2024, Accepted: 10 Jan. 2024

ABSTRACT: Rainwater infiltration is one of the main triggering factors in slope failure. Therefore, exploring the unsaturated slope behavior is essential. However, studies generally ignored the impact of soil-water characteristic curve (SWCC) hysteresis caused by wet-dry cycles in engineering practice. SWCC measured in the drying process is commonly used to estimate slope behavior in the wet-dry cycle. Three soils of Toyoura sand, Hiroshima decomposed granite soil (Masado soil), and DL clay will be taken as examples to examine the infinite slope stability under the effect of SWCC hysteresis. Firstly, this research examines soils' SWCC and suction stress characteristic curves (SSCC). Then, the factor of safety (FOS) changes are further analyzed when suction stress is considered the confining pressure. The results indicate that FOS for soils with small cohesion and air-entry value is greatly affected by SWCC hysteresis. As the depth between the selected slip surface and slope surface increases, the disparity between FOSs calculated through wetting FOS and drying FOS will decrease sharply. Therefore, for shallow slope stability analysis, only using the SWCC measured during the drying process to evaluate the entire wet-dry cycle might lead to underestimating slope failure potentiality.

Keywords: Unsaturated soil, Suction stress, Hysteresis, Slope stability, Factor of safety

1. INTRODUCTION

As an island country, Japan consists of many islands and mountains. Storms caused by topography are one of the most common activities in the area. According to the report by the Ministry of Land [1], soil disasters exceed 1,000 cases per year, and there were even an astonishing 2,000 cases in 2019. Most soil disasters occurred between June and October. In this period, the climate conditions are precarious, and it must consider the impact of rainwater infiltration on unsaturated slopes. This study will use Toyoura sand, Hiroshima decomposed granite soil (Masado soil), and DL clay to examine unsaturated slope stability under variable rainfall conditions.

As the most crucial property of unsaturated soil, the soil-water characteristic curve (SWCC) describes the relationship between soil moisture and matric suction. Generally, the increase in suction will cause a decrease in soil moisture. However, even for the same soil, suctions corresponding to the same soil moisture are different under the drying and wetting processes [2]. It can be observed that SWCC measured from the wetting process is always lower than that from the drying process, which is known as SWCC hysteresis. Tao et al. [3] examined the influence of the SWCC hysteresis effect during the drying-wetting cycle from the perspective of porosity and internal friction angle. Theoretically, SWCC hysteresis behavior will have a specific influence on calculations of FOS, but it is rarely discussed in existing studies. Generally, researchers prefer to use drying SWCC to estimate the slope behavior throughout the entire dryingwetting cycle, and the main reasons are speculated to be as follows:

- 1. One of the most commonly used methods for plotting SWCCs is to fit experimental data through mathematical models, such as the van Genuchten, Fredlund-Xing, or Brooks-Corey models [4-6]. However, these models do not involve the SWCC hysteresis in the extensive suction range. Although studies proposed some models that can be used to compute SWCC hysteresis impact due to complex calculations and inconvenient uses, these methods are rarely mentioned in practice calculations.
- 2. In the laboratory environment, measurement of soil suction is relatively easy. Generally, SWCC can be obtained through the tension meter, pressure plate, or filter paper. To show the impact of hysteresis, the wetting SWCC and drying SWCC must be measured over an extensive suction range. However, various difficulties and high costs in the above methods limit the analysis of SWCC hysteresis. As a result, drying SWCC is usually used to estimate the soil behavior in the entire wetdry cycle.

On the other hand, some research has recently explored SWCC hysteresis's impact on slope stability [7, 8]. However, these studies were usually performed with a single soil, and the results may differ for altering soil properties. One of the essential factors is the hydraulic conductivity (κ). Generally, κ for drying process is higher than the κ for wetting process, and it is not a constant value.

The wet front and infiltration rate may differ when analyzing slope stability through drying SWCC and wetting SWCC. This difference varies by soil type. Therefore, the simulated factor of safety (FOS) may be misjudged. This study will research the disparity between drying FOS and wetting FOS corresponding to the same saturation.

2. RESEARCH SIGNIFICANCE

This paper will take the infinite slope as an example to evaluate the influence of SWCC hysteresis on the FOS, considering the suction stress as the confining pressure. Then, the influence of different soils is examined by comparing three typical soils. This paper will further explore the effect at different depths and try to find the depth where the SWCC hysteresis impact reaches maximum. This conclusion can be extended to finite slopes and provide the theoretical judgment basis for actual engineering.

3. CALCULATION MODE

When analyzing the slope stability, the limit equilibrium method (LEM) and the numerical analysis method are the most commonly used methods. The limit equilibrium method assumes that the slope has a sliding surface and is in a state of limit equilibrium. Then, discretize the slope into soil slices with vertical boundaries and analyze the static force equilibrium or bending moment equilibrium. The essence of the numerical analysis method is the unit discretization that, the slope can be split into several grid units, and the stress state of each element can be computed by finite element method (FEM), boundary element method (BEM), or discrete element method (DEM) [9].

In practical operation, the limit equilibrium method is much simpler than the numerical analysis method. Much of the existing literature adopts the Fellenius method [10] or Bishop's simplified method [11] to analyze slope safety status. In LEM, the factor of safety (FOS) is the most significant parameter. The definition equation is $F = \frac{\tau_f}{\tau}$, where F is the FOS; τ_f is the shear strength of the soil on the sliding surface, and τ refers to the sliding force on the slope. Generally, the slope will keep stable with the large FOS. If the FOS is less than 1.0, the slope will be in unstable state. To obtain the FOS, the shear strength of the soil must be resolved.

3.1 Effect of Suction Stress as The Confining Pressure

The general equations for the shear strength of unsaturated soil can be considered as the extension of effective stress (skeleton stress) equation proposed by Bishop [12]:

$$\sigma' = (\sigma - u_a) + (u_a - u_w)\chi \tag{1}$$

where σ' is the Bishop's effective stress; σ is the total stress; u_a is the pore-air pressure; u_w is the pore-water pressure; $\sigma - u_a$ is the net stress; χ is parameter related to soil saturation. On this basis, the shear strength of unsaturated soil is given through Mohr's failure criterion:

$$\tau = c' + (\sigma_n - u_a) \tan \varphi' + (u_a - u_w) \chi \quad (2)$$

where c' is the effective cohesion of soil; φ' is the internal friction angle.

As mentioned above, various prediction models can be employed to compute the "effective stress" defined by Bishop [12], and the structures of the equation are generally similar. The main difference lies in calculating the shear strength contributed by suction. In this study, the model proposed by Vanapalli et al. [13] will be used to calculate the shear strength of unsaturated soil:

$$\tau_{f} = c' + (\sigma_{n} - u_{a}) \tan \varphi' + (u_{a} - u_{w}) \times \left[(\tan \varphi') \left(\frac{\theta_{w} - \theta_{r}}{\theta_{s} - \theta_{r}} \right) \right]$$
(3)

or

$$\tau_f = c' + (\sigma_n - u_a) \tan \varphi' + (u_a - u_w) \times \left[(\tan \varphi') \left(\frac{S - S_r}{100 - S_r} \right) \right]$$
(4)

where θ_w and S are the current volumetric water content and degree of saturation, respectively; θ_r and S_r are the volumetric water content and degree of saturation in the residual state, respectively.

model can capture the characteristics of the shear strength when the volumetric water content or saturation varies. However, it cannot simulate the shear stress change well when the water content exceeds the residual zone (S<Sr). For this study, the critical point is the impact of changes in soil water moisture on shear strength, and the SWCC hysteresis effect does not involve the situation where the soil reaches the residual state. Therefore, the model is available to predict the soil behavior with the soil moisture changes. On this basis, Karube et al. [14] summarized the contribution of suction to shear strength as suction stress. As shown:

$$p_s = S_e * s = \frac{S - Sr}{(100 - Sr)} * s$$
 (5a)

$$p_s = S_e * s = \frac{\theta_w - \theta_r}{\theta_s - \theta_r} * s \tag{5b}$$

where S_e is the effective saturation; s is the suction.

On this basis, experiments conducted by Kato et al. [15] indicated that the suction stress (p_s) in unsaturated soil can also be considered as part of the confining pressure to further increase the shear strength rather than only as the cohesion component.

In detail, if the analysis is carried out according to Eq. (3) or Eq. (4), the suction stress will only be considered part of the cohesion. In this case, when performing the unconfined compression test on the unsaturated soil, the Mohr's circle should be tangent to the Y axis (like the UC test for saturated soil in Fig.1a). However, according to experiment results of the unconfined compression test on unsaturated soil [15], the distance appears between the experimentally obtained Mohr's circle and the Y axis (Fig.1b). And Kim et al. [16] proved that this distance is equal to the suction stress (p_s) through geometric verification.

Therefore, it can be considered that the p_s in unsaturated soil is not only a part of the cohesion but also contributes to the shear strength as a part of the confining pressure. Then, the formula can be modified as follows:

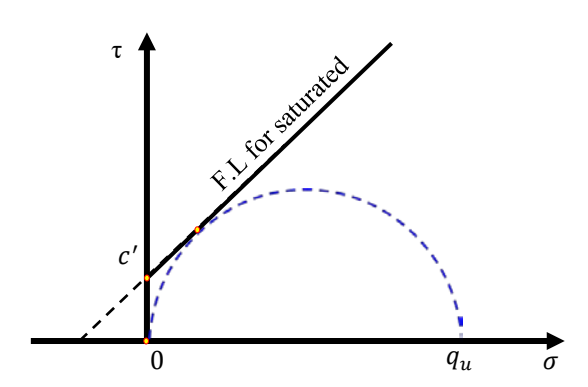


Fig.1a Unconfined compression test for saturated soil

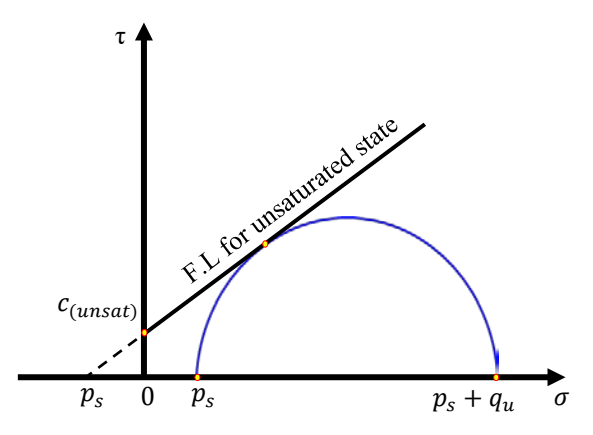


Fig.1b Unconfined compression test for unsaturated soil

$$\tau_f = c' + (\sigma_n - u_a + p_s) \tan \varphi' + (u_a - u_w) \left[(\tan \varphi') \left(\frac{S - S_r}{100 - S_r} \right) \right]$$
 (6)

However, the contribution of suction stress to the FOS has rarely been studied. Therefore, under the condition of p_s acting as confining pressure, the influence of the wet-dry cycle on FOS deserves further discussion.

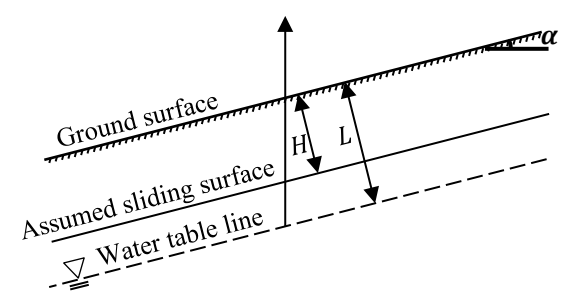


Fig.2 Diagram of an infinite slope

3.2 Factor of Safety of Unsaturated Infinite Slope

This paper will analyze the assumed homogeneous infinite unsaturated slope (Fig. 2). When the sliding surface is in the soil layer with depth H, its FOS can be expressed as [17]:

$$F_s = \frac{c_s + (\sigma_n - u_a) \tan \varphi'}{\gamma_t H \sin \alpha} \tag{7}$$

where: F_s is the safety factor; c_s is the total cohesion of soil, including cohesion of saturated part c' and the contribution of suction stress to cohesion in the unsaturated part; γ_t is the volumetric weight of the soil; H is the depth of sliding surface below the ground surface; α is the angle of the slope. Then, as described in Eq. (6), since there is another suction stress as an additional confining pressure, the equation could be modified into:

$$F_{s} = \frac{c_{s} + (\sigma_{n} - u_{a} + p_{s}) \tan \varphi'}{\gamma_{t} H \sin \alpha}$$
 (8)

And for the theoretically infinite slope, the forces between the slices can be ignored, and the normal stress perpendicular to the slope come from the component of gravity, that is:

$$\sigma_n - u_a = \gamma_t H \cos \alpha \tag{9}$$

Therefore, Eq. (8) can be rewritten as:

$$F_{s} = \frac{C_{s}}{\gamma_{t} H \sin \alpha} + \frac{\tan \varphi'}{\tan \alpha} + \frac{p_{s} \tan \varphi'}{\gamma_{t} H \sin \alpha}$$
 (10)

4. ANALYSIS OF LIMIT EQUILIBRIUM STATE

For the theoretical evaluation of general slope, force balance and moment balance analysis at the limit equilibrium state is one of the most popular methods. The method can also be extended by adding other factors such as earthquake, water pressure, or modification of parameters according to the actual situation.

Compared with Cho and Lee's method [17], it has more flexibility. Since the limit equilibrium analysis method is not the assumed infinite slope, the requirement of soil slices could be adjusted according to the actual slope size. Due to its complex calculation, computer software is usually employed for the analysis. In this research, SEEP/W will be used to simulate the rainfall infiltration [18]. For analysis of rainfall penetration problems through SEEP/W, slope geometry, boundary conditions, and soil properties are required. The flux situation on the slope surface could be controlled by altering boundary conditions. Runoff could be simulated when rainfall occurs by providing zero constant water pressures to the slope surface. Moreover, pore-water pressure distribution could be obtained at different times and positions.

Further, LEM is used in SLOPE/W to determine the FOS [19]. The basic calculation logic is as follows:

According to the definition of FOS: $F = \tau_f/\tau$, the reduced shear strength of soil slice (mobilized shear force) can be given as:

$$\tau_m = \frac{\beta \tau}{F} = \frac{\beta}{F} [c_s + (\sigma_n - u_a + p_s) \tan \varphi']$$
 (11)

where τ_m is the mobilized shear force; τ_f is the shear strength; τ is the shear stress; F is the factor of safety; β is the projection of the width of the soil slice on the bottom of the slip surface; $\sigma_n = \frac{N}{\beta}$ is the average normal stress perpendicular to the sliding surface. Therefore, the equilibrium equation of each soil slice could be written according to the moment balance and force balance respectively:

Taking the circle center of the sliding surface as the reference for moment equilibrium:

$$Wx_W + E_L x_{E_L} - E_R x_{E_R} + X_L x_{X_L} - X_R x_{X_R} - \tau_m x_{\tau_m} - Nx_N = 0$$
 (12)

Force equilibrium in the horizontal direction:

$$E_L - E_R - \tau_m \cos \alpha - N \sin \alpha = 0 \tag{13}$$

where W is the self-weight of each soil slice; N is the normal force on the base of the slice; x_i is the distance from each force to the circle center of the

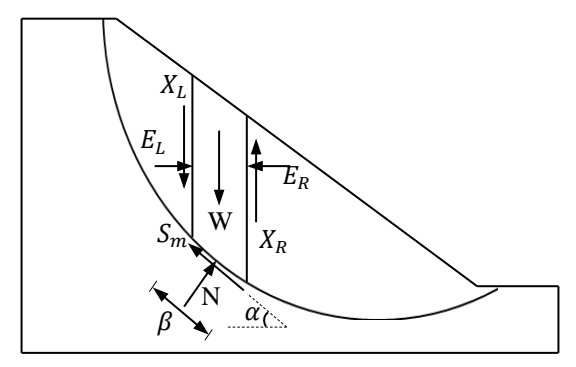


Fig.3 Force Analysis for the 2-D Slope

slip surface; E_L , E_R , X_L , X_R are the horizontal compression force and vertical shear force caused by the soil slices adjacent to the selected soil slice, respectively (mark "L" is left and mark "R" is right). The equation describes the force situation of one soil slice. Since all soil slices will be summed in subsequent calculations, the forces E and X can be considered as the state of mutual cancellation under the condition of no external force.

$$F_m = \frac{\sum \beta R[c_s + (\sigma_n - u_a + p_s) \tan \varphi']}{\sum W x_W - \sum N x_N}$$
(14)

$$F_f = \frac{\sum \beta \cos \alpha \left[c_s + (\sigma_n - u_a + p_s) \tan \varphi' \right]}{\sum N \sin \alpha}$$
(15)

In practice cases, the shear forces X and normal stress E in selected soil slices are difficult to solve. External methods are necessary to calculate the average normal stress perpendicular to the contact surface (N). This research will adopt the simplified Bishop method to obtain the FOS. The normal stress E and shear force X between soil slices can be ignored. Therefore, normal stress can be considered as $N = W \cos \alpha$.

Note that if the moment equilibrium equation and force equilibrium equation are analyzed in infinite slope through Eq. (14) and Eq. (15), the sliding surface will be a straight line parallel to the slope, and the "circle center" of the slip surface will be considered as a point located at infinity perpendicular to the contact surface. Therefore $x_N = 0$, and Eq. (14) and Eq. (15) are consistent with Eq. (10).

In Geostudio, Eq. (3) or Eq. (4) are generally used to analyze the slope stability by SEEP/W and SLOPE/W. It does not consider the contribution of suction stress acting as the confining pressure. Therefore, $F_m = F(s) + F(p_s)$ can be used to modify the FOS:

$$F(s) = \frac{C_s}{\gamma_t H \sin \alpha} + \frac{\tan \varphi'}{\tan \alpha}$$
 (16)

and:

$$F(p_s) = \frac{p_s \tan \varphi'}{\gamma_t H \sin \alpha} \tag{17}$$

Where F_m is the FOS with considering p_s as the confining pressure; F(s) is the FOS calculated by Geostudio; and $F(p_s)$ is the correction value of FOS that needs to be calculated additionally.

5. SOIL PARAMETERS AND DATA PROCESSING

In this study, the selected soil objects are Toyoura sand, Massa soil, and DL clay. Hatakeyama et al. [20] conducted continuous pressurization and stage pressurization experiments on the three kinds of soils to obtain the experimental soil-water characteristic curves. Soil parameters are shown in Table 1.

Table 1 Basic parameters of soils

Tested soils	Particles Density (g/cm³)	Uniformity Coefficient U_c	Mean Grain Diameter $D_{50}(mm)$
Toyoura sand	2.641	1.49	0.172
Masado soil	2.614	46.1	0.484
DL clay	2.651	4.58	0.0171

These three kinds of soil present typical sand, clay, and silt. The particles of Toyoura sand are relatively large, and the size is around 0.1mm, which can be considered as soil with poor water retention performance. The average particle size distribution (PSD) of DL clay is nearly 0.01mm, and water retention performance is much stronger than that of Toyoura sand; Masado soil is a fine-grained material with a comprehensive PSD. The infinite slope composed of these three soils will theoretically explore the influence of the SWCC hysteresis on slope FOS.

The SWCC of the wetting process and drying process are calculated by extracting the points of the pressurization experiment from Hatakeyama et al. [20], and the SWCC model proposed by Van Genuchten [4] will be used to fit the experimental result:

$$S_e = \left\{ \frac{1}{1 + \left[a(u_a - u_w) \right]^n} \right\}^{1 - \frac{1}{n}} \tag{18}$$

where a and n are fitting parameters; a is approximately the reciprocal of the air-entry value; n is related to the void distribution of the soil. Combined with Eq. (5), the relationship between suction and volumetric water content can be obtained:

$$\theta_{w} = \left\{ \frac{1}{1 + \left[a(u_{a} - u_{w}) \right]^{n}} \right\}^{1 - \frac{1}{n}} * (\theta_{s} - \theta_{r}) + \theta_{r}(19)$$

Then, plot the suction stress characteristic curve (SSCC), that is, the relationship between suction stress (p_s) and suction [21,22]. The fitting parameter and the obtained SWCC and SSCC are shown in Table 2 and Fig.4, respectively:

Table 2 SWCC parameters of soils for V-G model

	Toyoura	Masado	DL
	sand	soil	clay
$\rho_d (g/cm^3)$	1.5	1.08	1.5
$a_d (kPa)$	0.25	2.6	0.03
$a_w(kPa)$	0.44	5.12	0.04
n_d	5.0	1.80	2.33
n_w	4.1	1.6	2.36

Manually calculate factor of safety of the homogeneous two-dimensional infinite slope first. Set the distance between the selected slip surface and the ground surface as H. The soil parameters in the slope are the same as mentioned above. Then compare the results of the four cases in Table 3: Case 1: suction stress (p_s) only acts as cohesion in drying process; Case 2: suction stress p_s only acts as cohesion in wetting process; Case 3: p_s contributes to confining pressure in drying process; Case 4: p_s contribute to confining pressure in wetting process.

Table 3 Marks for different cases

	p_s only acts as cohesion	p_s contributes to confining pressure
Dry SWCC	CASE 1	CASE 3
Wet SWCC	CASE 2	CASE 4

6. RESULT AND DISCUSSION

6.1 Effect of Saturation on Suction Stress

The SSCC characteristics of Toyoura sand, Masado soil, and DL clay correspond to the typical SSCCs for sand, clay, and silt in Fig.5, respectively [23]. As the applied suction is smaller than the air-entry value (AEV), the soil will keep the stage fully saturated, and the suction stress is equal to the applied suction. When soil saturation begins to decrease, the changes in suction stress of Toyoura sand and DL clay are different from Masado soil.

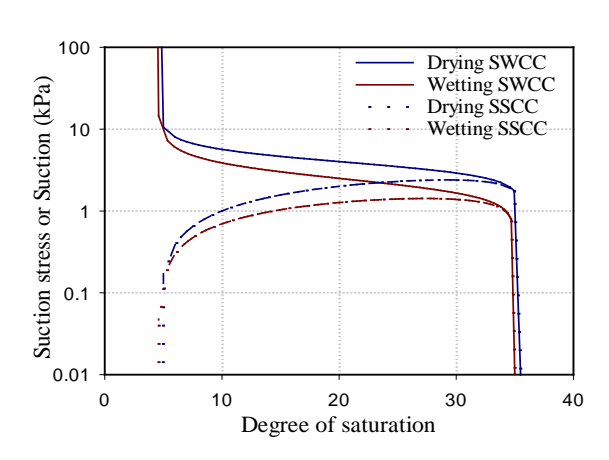


Fig.4a SWCC and SSCC for Toyoura sand

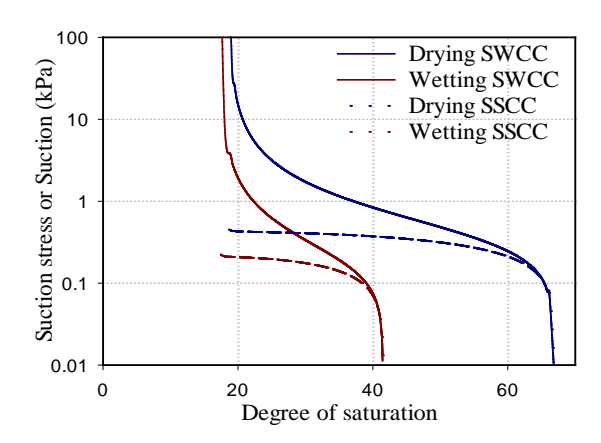


Fig.4b SWCC and SSCC for Masado soil

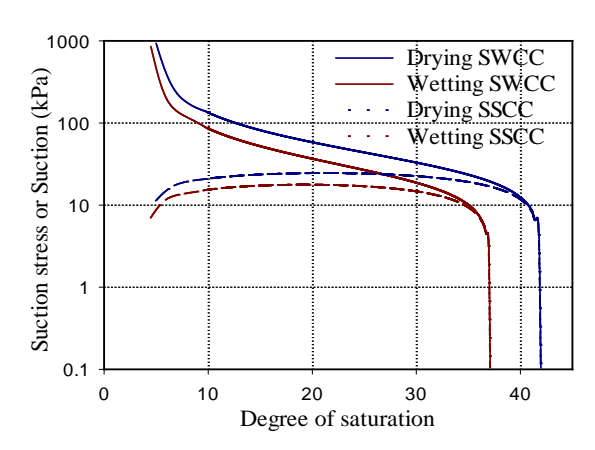


Fig.4c SWCC and SSCC for DL clay

For Toyoura sand and DL clay, a decrease in saturation will cause a decrease in suction stress, but the suction stress of Masado soil will remain nearly constant

Furthermore, the SSCC of Masado soil contains an indistinct residual zone, indicating that even at the high suction zone, the continuity of the water phase remains. The behavior of Masado soil in this

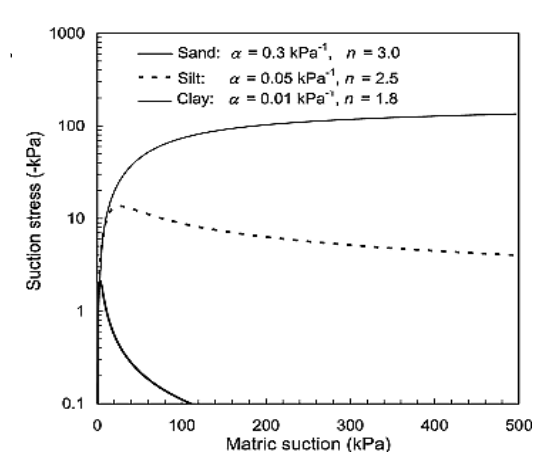


Fig.5 SWCC for 3 soils (From Lu [23].)

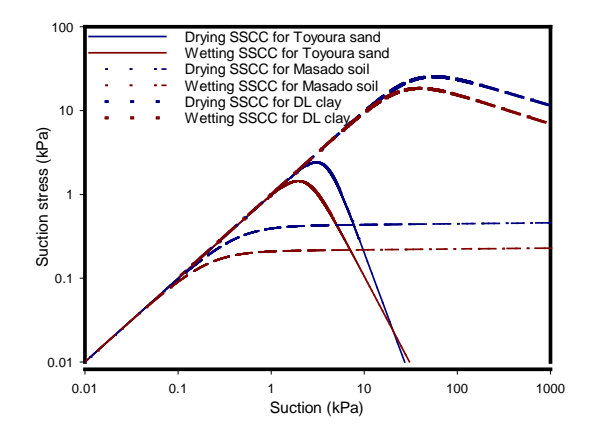


Fig.6 SSCCs for 3 soils

research agrees with the results of clay soil observed by other studies [24,25].

Fig.4 and Fig.6 compare the SWCCs and SSCCs in the drying and wetting processes. In high saturation or low suction areas, the difference between suction stress (drying suction stress) corresponding to the drying process and the suction stress (wetting suction stress) corresponding to the wetting process cannot be observed. With the decrease in soil saturation (or increase in suction) for Toyoura sand and DL clay, the impact of SWCC hysteresis will increase to maximum, then decrease to 0. According to the Fig.6, the inflection point is around AEV or WEV (Water-entry value). For Masado soil, when the impact of SWCC hysteresis peaks, a decrease in soil saturation will not affect the difference between the two curves, and the wetting curve will be parallel to the drying curve.

6.2 Effect of suction stress on FOS

The example is to examine the infinite slope behavior under the influence of SWCC hysteresis. In the established model, the distance between the selected surface and the ground surface is set to 1 meter(H=1m); The angle of infinite slope is set to

26°; Eq. (14) and Eq. (15) are used to compute FOSs of case 1,2 and case 3,4 in table 3, respectively. The plotted profile is shown in Fig.7.

Similar to SSCCs, the FOS disparity of Toyoura sand or DL clay decreases when suction exceeds AEV. On the other hand, the clay of Masado soil's FOSs of each case will remain around a constant value even if suction is greater than AEV. The trend of the relationship curve between FOS and suction is almost identical to that of SSCCs for all three soils, indicating that suction stress plays an essential role in FOS changes. In the monotonic drying or wetting process, since FOS_{case3} and FOS_{case4} add another suction stress as the confining pressure based on the FOS_{case1} and FOS_{case2}, the impact of SWCC hysteresis will further increase.

For Toyoura sand and DL clay, when the suction is near AEV, SWCC hysteresis impacts in FOS are around 15% and 30%, respectively. For Masado soil, the difference between wetting FOS and drying FOS will not exceed 0.1, nearly 3%. Soil properties can be considered as one of the most critical factors. Since the AEV of the selected Masado soil is only 0.68kPa, the increase in suction stress is limited based on the characteristics of typical clay's SSCC, and the maximum value is only 0.4kPa. However, the cohesion of Masado soil is set to 5kPa in the shear strength calculation. Compared with cohesion, the influence of suction stress on FOS is diluted. The cohesion is generally low for Toyoura sand and DL clay, and it can be directly set to 0. Hence, the influence on FOSs is apparent. Therefore, the impact of SWCC hysteresis is not apparent for soil with high cohesion.

6.3 Effect of cases on FOS at different depths

parameter settings for simulation

This study employed Geostudio to simulate the infinite slope behavior. The established model is shown in the Fig 8. The solid line in the model is the ground surface, and five dotted lines represent five cases of distances between sliding surfaces. The ground surface is 1m, 3m, 5m, 10m, and 15m, respectively. Then, the "Fully specify slip surface" command and the "Tension crack line" command can be used to create the soil slices possessing the same thickness and going vertically upwards. The sliding surface of the infinite slope can be simulated [19]. In simulation, the rainfall condition is set to be 50mm/h for 10 days and continuous drainage for 20 days. To reduce the influence on the initial state, the water level line is set parallel to the slope and close to the bottom.

The study is to explore the difference between wetting FOS and drying FOS under the same water content. For soils like the Toyoura sand used in this research, FOS will be sensitive to rainwater infiltrates due to small AEV and large hydraulic

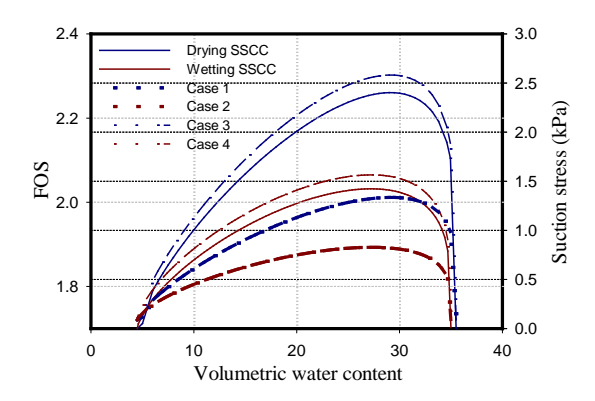


Fig.7a Relationship between FOS and suction for Toyoura sand

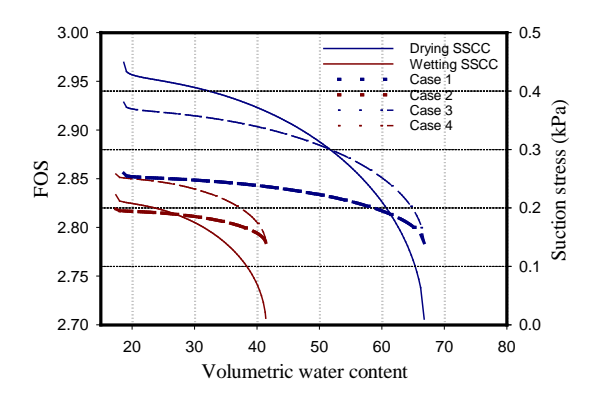


Fig.7b Relationship between FOS and suction for Masado soil

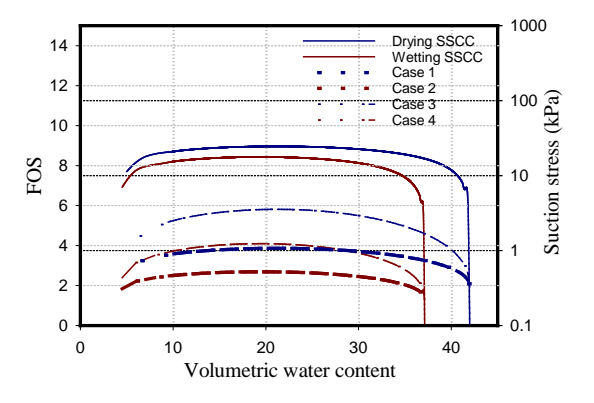


Fig.7c Relationship between FOS and suction for DL clay

conductivity (κ) in wetting and drying processes. The impact of SWCC hysteresis on FOS is difficult to observe. Further, the changes in κ of different cases are not the same. Therefore, simulation with the actual soil parameter is complex to analyze. To mitigate the interference, in this simulation, the κ is adjusted adequately for different soils to defer the rate of rainwater infiltration. Moreover, the

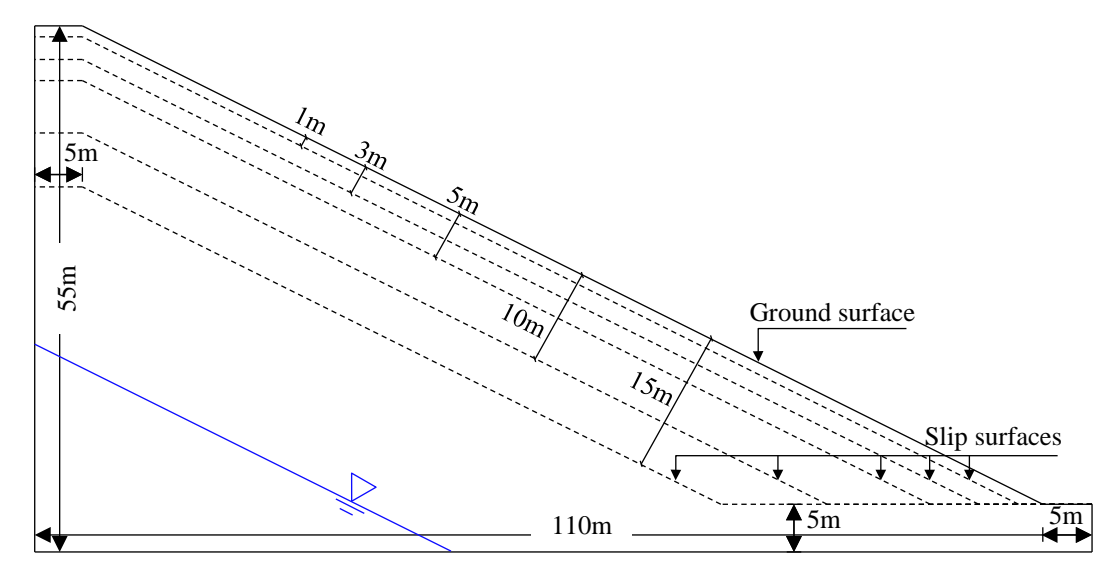
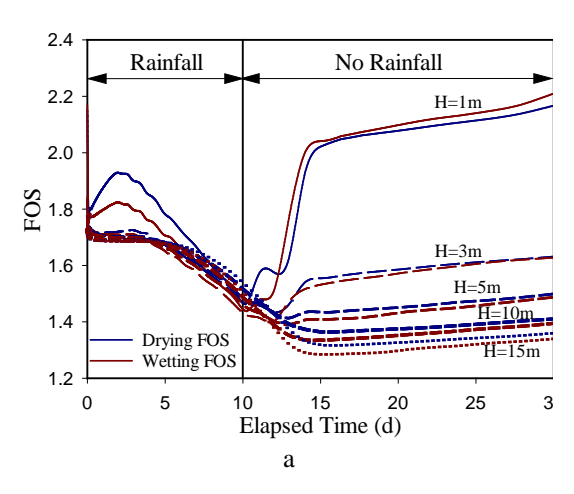
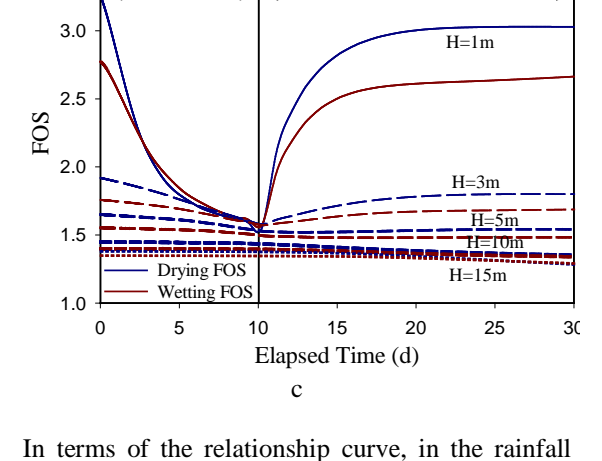


Fig.8 The model used for the simulation

3.5

Rainfall

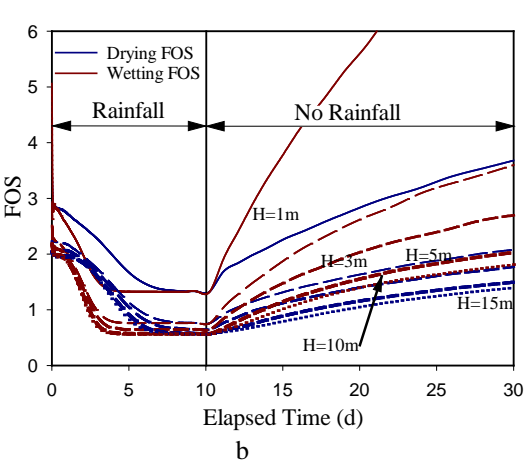




stage, as the saturation increases, the factor of safety simulated by the SWCC of the wetting process

(wetting FOS), and the factor of safety simulated by the SWCC of the drying process (drying FOS) of

No Rainfall



Elapsed Time (d) conclusion obtained fro According to Fig. 8, κ close to the ground sur difference of FOSs under different cases can be observed perceptibly. Simultaneously, the κ of each soil is set to a constant value to avoid errors caused by different infiltration rates. The results are shown

Result and discussion for simulation

in Fig.9.

the three types of soils all show a decreasing trend. However, in the wetting process, the decreasing range of wetting FOS is always greater than that of drying FOS, and the gap always maintains a process of increasing and then decreasing. When the slope tends to be saturated, the impact of the wet-dry cycle on the FOS is minimized. That is, the two FOS are almost equal, which is consistent with the conclusion obtained from the theoretical calculation. According to Fig. 8, when the sliding surface is close to the ground surface, the more considerable difference between the drying FOS and the wetting FOS will occur with the saturation change. Specifically, when the distance between the sliding surface and the ground surface is H=1m, the FOS differences of Toyoura sand, Masado soil, and DL clay are about 10%, 40%, and 15%, respectively. When the H reaches 3 meters, the gap will drastically

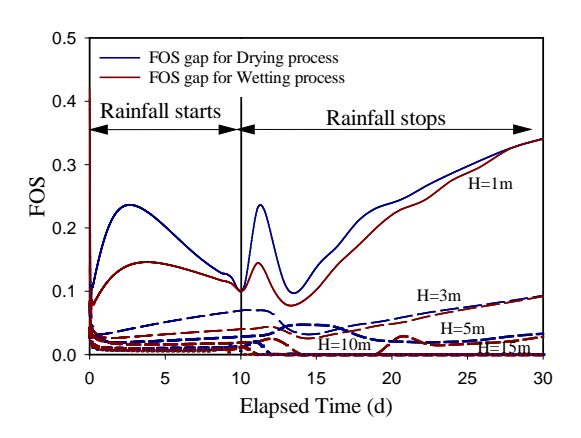


Fig. 10a Relationship between FOS gap and time for Toyoura sand

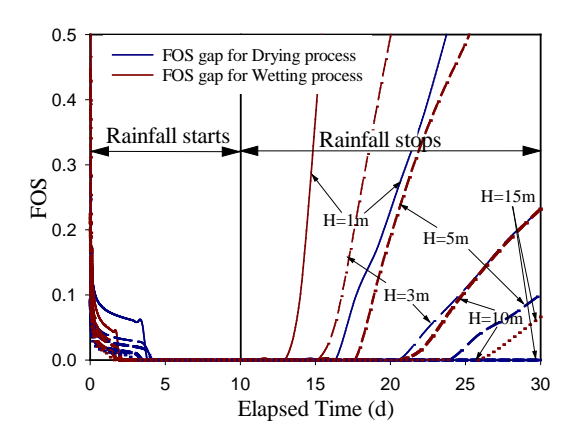


Fig.10b Relationship between FOS gap and time for Masado soil

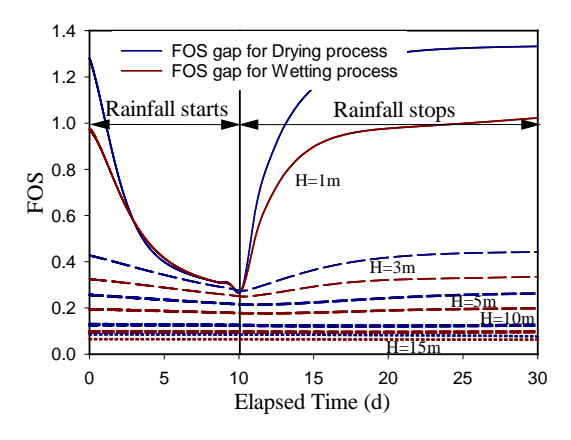


Fig.10c Relationship between FOS gap and time for DL clay

reduce to 3%, 30%, and 8%. However, if the depth is further increased to 5m, 10m, or 15m, the differences between the drying FOS and the wetting FOS of the three soils become negligible. Furthermore, at depths greater than 5m, FOSs

appear to be less sensitive to the changes in saturation throughout the wet-dry cycle.

Simultaneously, as mentioned above, Eq. (17) could be used to compute $FOS_{case3} - FOS_{case1}$ and $FOS_{case4} - FOS_{case2}$, and the "gap curve" could be plotted (Fig.10). The gap curve shows a similar change trend with FOS changes in Fig.9. Compared with case 1 and case 2, case 3 and case 4 can provide more FOS, especially when the selected slip surface is close to the slope surface. However, with the increase in depth between the selected slip surface and ground surface, the FOSs obtained by the two calculation methods tend to be the same.

Therefore, for slopes with a large distance between the slip surface and the ground surface, the obtained FOSs in the four cases are similar. However, for shallow slopes with a depth of less than 5m, the hysteresis effect of SWCC and the contribution of p_s acting as the confining pressure will have a particular impact on slope FOS, and specific analysis is required.

7. CONCLUSION

This paper first analyzed the influence of hysteresis on the soil water characteristic curve (SWCC). Then, the experimental data of Toyoura sand, Masado soil, and DL clay obtained by Hatakeyama et al. [20] were cited to examine suction stress characteristic curves (SSCC), And the impact of suction stress acting as confining pressure was evaluated. On this basis, Geostudio was used to simulate the infinite slope behavior to expand the results:

- 1. SSCCs were compared with the relationship between FOS and suction in the infinite slope at the depth H=1m. Suction stress can be considered to dominate the changes in FOS. Moreover, the difference between FOSs obtained by wetting SWCC and drying SWCC will further increase when p_s is considered as extra confining pressure.
- 2. The SSCCs of the three soils are different in wetting and drying processes. Soils with low c', such as Toyoura Sand and DL clay, are greatly affected by SWCC hysteresis. In Masado soil, since the c' is set to 5kPa, the influence of the suction stress on FOS is diluted.
- 3. Geotechnical software, Geostudio, is used to simulate the slope behavior at various depths. Results show that when the selected H is less than 5 m, slope stability will be significantly affected by SWCC hysteresis and p_s acting as confining pressure. Moreover, as the H continues to increase, this effect will be weakened rapidly.

Overall, in the previous slope stability analysis, the hysteresis effect of SWCC was usually ignored. Only the SWCC obtained from the drying process

was used to estimate the soil behavior in a wet-dry cycle. This study examined that the treatment may be suitable for slopes with large distances from the selected sliding surface to the ground surface. However, it may seriously underestimate the impact of SWCC hysteresis and p_s acting as confining pressure for shallow slopes.

8. REFERENCES

- [1] Ministry of Land, Infrastructure, Transport and Tourism, Occurrence of sediment-related disasters in 2019.
- [2] Rahardjo H., Heng O.B., Choon L.E., Shear strength of a compacted residual soil from consolidated drained and constant water content triaxial tests. Canadian Geotechnical Journal, Vol. 41, Issue 3, 2004, pp.421-436.
- [3] Tao G., Li Z., Liu L., Chen Y., Gu K., Effects of Contact Angle on the Hysteresis Effect of Soil-Water Characteristic Curves during Dry-Wet Cycles. Advances in Civil Engineering, vol. 2021, Issue 2, 2021, pp. 1-11.
- [4] Van Genuchten, M.Th., A closed-form equation for predicting the hydraulic conductivity of unsaturated soils. Soil Science Society of America Journal, Vol. 44, Issue 5, 1980, pp. 892–898.
- [5] Fredlund D. G., and Xing A., Equations for the soil-water characteristic curve. Canadian Geotechnical Journal, Vol. 31, Issue 4, 1994, pp. 521–532.
- [6] Brooks R. H., and Corey A. T., Hydraulic properties of porous media. Hydrology papers (Colorado State Univ.,), 1964, pp.1-11.
- [7] Chen P., Mirus B., Lu N., Godt J.W., Effect of hydraulic hysteresis on stability of infinite slopes under steady infiltration. J. Geo-tech. Geoenviron. Eng. Vol. 143, Issue 9, 2017, pp. 1-10
- [8] Kristo C., Rahardjo H., Satyanaga A., Effect of hysteresis on the stability of residual soil slope. Int. Soil Water Conserv. Res. Vol. 7, Issue 3, 2019, pp. 226–238.
- [9] Pourkhosravani A., Kalantari B., A review of current methods for slope stability evaluation. Electron. J. Geotech. Eng. Vol. 16, 2011, pp. 1245–1254.
- [10] Fellenius W., Calculation of the Stability of Earth Dams. Trans. 2nd Int. Cong. Large Dams, Washington DC, Vol. 4, 1936, pp. 445-462.
- [11] Bishop A. W., The use of the Slip Circle in the Stability Analysis of Slopes. Géotechnique. Vol. 5, Issue 1, 1955, pp. 7–17.
- [12] Bishop A. W, Blight G. E., Some aspects of effective stress in saturated and partly

- saturated soils. Geotechnique, Vol. 13, Issue 3, 1963, pp. 177–97.
- [13] Vanapalli S. K., Fredlund D. G., Pufahl D. E., and Clifton A. W., Model for the prediction of shear strength with respect to soil suction. Canadian Geotechnical Journal. Vol. 33, Issue 3, 1996, pp. 379-392.
- [14] Karube D., Kato S., Hamada K. and Honda M., The relationship between the mechanical behavior and the state of pore water in unsaturated soil. J. Geotech. Engrg., Proc. of JSCE, Vol. 535, 1996, pp. 83-92.
- [15] Kato S., Yoshimura Y., Fredlund D. G., Role of matric suction in the interpretations of unconfined compression tests. Proceedings of the 58th Canadian Geotechnical Conference, Saskatoon, SK. Vol.2, 2005, pp. 410-415.
- [16] Kim B. S., Park S. W., Lohani T. N., Kato S., Characterizing suction stress and shear strength for unsaturated geomaterials under various confining pressure conditions. Transp. Geotech. Vol. 34, Issue. 4, 2022, pp. 1-11.
- [17] Cho S. E., and Lee S. R., Evaluation of surficial stability for homogeneous slopes considering rainfall characteristics. Journal of Geotechnical and Geoenvironmental Engineering, Vol. 128, Issue 9, 2002, pp. 756–763.
- [18] Geo-Slope International Ltd. (2012a). Seepage modeling with SEEP/W. Calgary, Alberta: July 2012 Edition. pp.1-205.
- [19] Geo-Slope International Ltd. (2012b). Slope modeling with SLOPE/W. Calgary, Alberta: July 2012 Edition. pp.1-406.
- [20] Hatakeyama M., Kyono S., and Kawahara T., Development of Water Retention Test Apparatus According to the Continuous Pressurization Method. Oyo Technical Report, No.34, 2015, pp.23-54.
- [21] Kato S., Yoshimura Y., Kawai K., and Sunden W., Effects of suction on strength characteristics of unconfined compression test for a compacted silty clay. JSCE, Vol. 687, 2001, pp. 201-218.
- [22] Lu N., Likos W. J., Suction stress characteristic curve for unsaturated soil. Journal of Geotechnical and Geoenvironmental Engineering, Vol. 132, Issue 2, 2006, pp. 131–142.
- [23] Lu N., Godt J.W., Wu D.T., A closed-form equation for effective stress in unsaturated soil. Water Resources Research, Vol. 46, Issue 5, 2010, pp. 1-14
- [24] Fleureau J.M., Kheirbek-Saoud S., Soemitro R., Taibi S., Behavior of clayey soils on drying-wetting paths. Canadian Geotechnical Journal, Vol. 30, Issue 2, 1993, pp. 287-296.
- [25] Tripathy S., Bag R., and Thomas H. R., Desorption and consolidation behavior of

initially saturated clays. In Proceedings of the 5th International Conference on Unsaturated Soils, Barcelona. Edited by E.E. Alonso and A. Gens. Taylor & Francis, London. Vol. 1, 2010, pp. 381–386.

[26] Hu D.P. Evaluation of unsaturated slope stability under rainfall infiltration, Memoirs of

Construction Engineering Research Institute, Vol.65, 2023, pp. 9-19

Copyright \odot Int. J. of GEOMATE All rights reserved, including making copies, unless permission is obtained from the copyright proprietors.